The interpretation of plasma edge conditions in tokamaks

1985 Plasma Phys. Control. Fusion 27 1411

(http://iopscience.iop.org/0741-3335/27/12A/008)

Plasma Physics and Controlled Fusion, Vol. 27, No. 12A, pp. 1411-1425, 1985
Printed in Great Britain

0741-3335/85$3.00+ .00
Institute of Physics and Pergamon Press Ltd.

THE INTERPRETATION OF PLASMA EDGE CONDITIONS IN TOKAMAKS

G M McCracken and P C Stangeby*

Culham Laboratory, Abingdon, Oxon OX14 3DB, England
(Euratom/UKAEA Fusion Association)

*JET Joint Undertaking and Aerospace Institute,
University of Toronto, Canada

ABSTRACT

The modelling used in the boundary layer depends on a number of factors including whether energy loss is dominated by convection through the sheath, by conduction, or by radiation from impurities. A number of criteria are derived for assessing these factors and are then compared with the experimental data from a range of tokamaks. The comparison is limited to tokamaks operating with limiters, although the criteria also apply to tokamaks with divertors.

In most tokamaks, under normal operating conditions, the dominant impurity process is sputtering. Impurities from the wall and limiter enter as neutral atoms and undergo ionization at radial positions which depend on the boundary plasma density and temperature profiles. When impurity densities are sufficiently high they can reduce the edge temperature by increasing the radiation level resulting in a feedback effect on impurity production. The impurity source profiles and impurity transport in the boundary are discussed.

1. INTRODUCTION

The plasma boundary in a tokamak is determined by a solid limiter or a magnetic separatrix. Radially inside the boundary the magnetic surfaces are closed; radially outside they are open i.e. they intersect a solid surface. The energy flux to the boundary layer is determined by the input power less the power radiated. The temperature at the boundary is determined primarily by the ratio of the energy flux to the particle flux transported to the boundary.

Although a vigorous effort has been made in recent years to diagnose the boundary layer in tokamaks the behaviour of the plasma in this region is far from being clearly understood. This is partly due to the complexity of the geometry. Not only is there the inherent 3D geometry of the torus which leads to marked toroidal and poloidal variations of the plasma parameters, e.g. the neutral density and the impurity fluxes, but there are also the practical complications due to the vacuum vessel and the internal diagnostics which lead to local obstructions and a very non-uniform wall. The measurements which have been made are usually only local ones and there is therefore uncertainty as to how representative they really are. It is clear, therefore that precise comparisons of the edge plasmas in different tokamaks is not justified; general features can, however, be identified and compared.

As the field lines in the boundary layer actually connect with a solid surface one expects the conditions to be quite different to that in the main body of the plasma. There is, in the first place, a large parallel loss of particles and energy. The length of the field line connecting the plasma to the surface (known as the connection length L_c) plays an important role in determining the plasma conditions. Obviously this length will vary widely depending on the size of the tokamak, on the design of the limiter and on the safety factor q of the plasma. There are then the questions of how collisional the plasma is, whether there are ionisation sources in the boundary layer, and whether there are energy loss terms due for example to radiation or charge-exchange?

In the first section of the paper we derive some simple criteria for estimating the importance of collisionality, equipartition, ionisation and radiation and compare these

criteria with the data collected from a number of tokamaks. In the second part of the paper we discuss impurity production, impurity screening and transport. The emphasis in each case is on simple analytical approaches to illustrate, where possible, the essential physics.

2. CRITERIA FOR BOUNDARY CONDITIONS

(i) Parallel Field Temperature Gradients

Modelling of the boundary depends strongly on whether power flow along field lines is limited by heat conduction along the plasma column or by the flow across the thin sheath which separates the plasma column from the solid surface. We assume a 1D model along the field direction with the plasma at the null point having a density and temperature n_m and T_m and the plasma at the limiter having the corresponding values n_s and T_s. The heat conducted along the flux tube is given by

$$Q = \kappa_0 T^{5/2} \, dT_e/dx \tag{1}$$

and the heat transferred across the sheath is

$$Q = \gamma_{\parallel} n_s \, c_s k T_e \tag{2}$$

where κ_0 is the Spitzer thermal conductivity, c_s the ion sound speed given by $c_s = (k(T_e+T_i)/m_i)^{\frac{1}{2}}$ and $\gamma_{\parallel}$ is the energy transmission factor across the sheath for an ion-electron pair (Stangeby 1984).

Within the torus we have to take into account the transfer of heat across the last closed field line or separatrix. We assume this to be a constant value per unit length along the flux tube. The amount of heat conducted down the flux tube has to be transferred across the sheath of the limiter. By integrating (1) and comparing it with (2) it can be shown (Stangeby, 1985a) that for a significant temperature drop to be developed in the flux tube we must have

$$8\kappa_0 T^{5/2} < 7 L_c n_s c_s \tag{3}$$

We take $\kappa_0 = 31500/Z_{eff}$ ln Λ, (Spitzer, 1962) $\ln\Lambda = 13$, $\gamma_{\parallel} = 8$ and obtain for D^+ ions, the condition

$$L_c n_s Z_{eff}/T_e^{\,2} \gtrsim 1.10^{17} \text{ m}^{-2} \text{ eV}^{-2} \tag{4}$$

An interesting observation is that the density dependance in this criterion is not due to collisionality but because as the density increases the energy transmitted through the sheath increases. In equilibrium, this same energy must be transmitted along the flux tube and results in an increased temperature gradient. The boundary defined by equation (4) is plotted in Fig.1. For a given null point temperature as $n_s L_c$ increases the temperature gradient along the flux tube increases rapidly, as also seen in Fig. 1. Below the critical value of nL_c the rate limiting step for heat transmission is at the sheath and no significant temperature gradient exists along the flux tube.

The existance of a strong temperature gradient along the plasma column can be very beneficial if it is sufficently strong to reduce the ion impact energy at the surface to below the sputtering threshold.

The amount of heat actually transferred to the surface can be readily determined once n, T and the sheath transmission factor are known. If we again take $\gamma_{\parallel} = 8$ and arbitrarily assume that $L_c = 10$ m, we can plot lines of constant power density on Fig. 1. In general it is only possible to tolerate power densities below ~ 10 MW/m^2, and hence practical values of n_s and T_s are restricted to those below this curve.

(ii) Effectiveness of Equipartition Collisions

We now consider the equipartition of energy between ions and electrons. Under many conditions the dominant energy loss for electrons is the convective loss through the sheath.

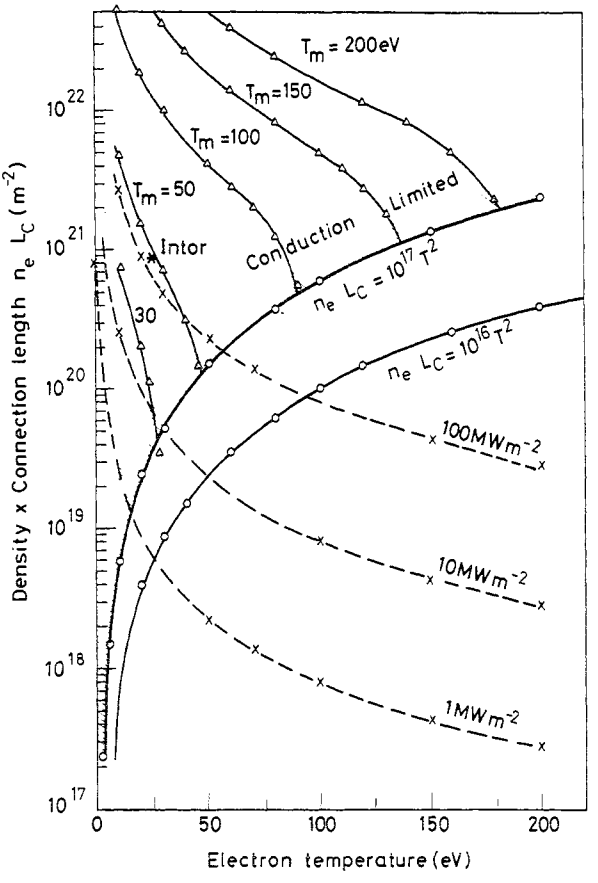

Fig. 1.

Criterion for a temperature gradient in the scrape off layer assuming no radiation loss. Above the line $n_e L_c = 10^{17} T^2$ there will be a temperature gradient, for $Z_{eff} = 1$.

The dotted lines show the power density for a given electron density and temperature. (L_c assumed = 10 m). Heat transfer considerations limit power densities to $\lesssim$ 10 MW m^{-2}.

For the electrons to be in equilibrium with the ions we therefore require that

$$k(T_i - T_e)\, \nu_{ie} n_e > n_s c_s\, (\gamma_{\parallel e} - 2)\, kT_e/2\, L_c \qquad (5)$$

where the left-hand side represents the usual expression for the transfer from ions to electrons. Using the usual form for the collision rate (Braginski, 1965)

$$\nu_{ie} = 3.2.10^{-15}\, Z^2 n_e \ln\Lambda / m_i T_e^{3/2}\ s^{-1} \qquad (6)$$

where m_i is the ion mass in amu. From equation (5) we obtain for deuterons

$$L_c n_e / T_e^2 \gtrsim 10^{17}\ m^{-2}\ eV^{-2} \qquad (7)$$

This interestingly is the same condition as we have above for conduction to be dominant, i.e. if one has a significant temperature gradient then $T_i \approx T_e$, (provided electron sheath cooling is the only important loss term).

(iii) Impurity Radiation as the Principal Energy Sink for Electrons

For radiation to be the main energy loss mechanism we must have

$$n_e n_z P_z > (\gamma_{\parallel} - 2)\, kT_e n_e c_s/2\, L_c \qquad (8)$$

where P_z is the radiation function i.e. the energy radiated per unit volume of impurity and

of electron density. Thus

$$n_z L_c > \gamma_{\parallel} kT_e c_s / P_z$$

Now usually the impurities in the boundary layer will be not be in coronal equilibrium. Calculation of the radiation constant for various plasma densities and confinement times (Carolan and Piotrowitz,1983) shows that in the range $10 < T < 300$ eV, for $n_e \tau_z < 10^{16}$ m^{-3} s, P_z is approximately constant $\sim 10^{-31}$ w m^3 for both carbon and oxygen. τ_z is the impurity dwell time in the scrape off layer. We thus obtain for deuterons

$$\frac{n_z L_c}{T^{3/2}} \gtrsim 5.10^{16} \text{ m}^{-2} \text{ eV}^{-3/2} \tag{9}$$

If radiation is the main energy loss mechanism then for equipartition to occur we must have

$$k(T_i - T_e)\nu_{ei} n_e \gtrsim n_e n_z P_z$$

$$kT\nu_{ei} \gtrsim n_z P_z$$

Using equation (6) for ν_{ei} and again taking $P_z \approx 10^{-31}$ w m^3 we obtain for carbon and oxygen

$$n_z/n_e \lesssim 0.1/T^{\frac{1}{2}} \tag{10}$$

We note that if we have a borderline case where impurity radiation and sheath cooling are equal then $n_z L_c/T^{3/2} = 5.10^{16}$ m^{-2} eV$^{-3/2}$ and

$$n_e L/T^2 \gtrsim 5\ 10^{17} \text{ m}^{-2} \text{ eV}^{-2} \tag{11}$$

for equipartition between ions and electrons

Clearly a radiation dominated boundary is beneficial since it means that energy is transferred from the core plasma over the large wall area, (about 200 m^2 on JET) rather than on the leading edge of the limiters (about 1m^2 in JET).

(iv) Collisions with Neutral Hydrogen

The presence of neutral hydrogen in the boundary layer, due for example to recycling or gas puffing, leads to ionization. The number of ions produced in the flux tube is given by

$$S = n_e n_g [\sigma v] L_c \text{ m}^{-2}\text{s}^{-1} \tag{12}$$

where $[\sigma v]$ is the rate coefficient for ionization of the gas.

If the number of ions produced by these collisions is comparable to the number flowing through the sheath, then we can say that it will significantly affect the particle balance. This condition can thus be written as

$$n_e n_g [\sigma v] L_c \sim 0.25\ n_e c_s \tag{12}$$

$$\text{i.e. } n_g L_c > c_s/[\sigma v]$$

Now for deuterons $c_s \approx 10^4 \sqrt{T_e}$ m s^{-1}, and a reasonable approximation for the rate coefficient for ionization is $[\sigma v] = 3.10^{-15} T^{\frac{1}{2}}$ m^3 s^{-1}; hence we obtain the condition for ionization to affect the particle balance to be

$$n_g L_c \gtrsim 3.10^{18} \tag{13}$$

In the absence of detailed modeling of the neutral particles in the edge one may use $n_g/n_e \sim 10^{-2}$. (Assume the refuelling is by Franck-Condon atoms of velocity $V_{FC} = 10^4$ ms^{-1}, then particle balance gives $V_{FC}\ n_g \approx D_\perp n_e/\lambda$ where λ is the plasma scrape off length in the edge, and $D_\perp$ is the plasma cross field diffusion coefficient. Typically $D_\perp \approx 1$ m^2 s^{-1}, $\lambda \approx 10^{-2}$ m, hence $n_g/n_e \approx 10^{-2}$.)

Even when ionization makes an appreciable contribution to the particle balance it usually does not significantly affect the energy balance. This is because energy loss is normally dominated by the sheath. The sheath removes $\gamma_{\|}$ kT ~ 10kT for each new ion pair created in the boundary layer, while the inelastic losses are < 3kT, provided T > 10 eV, (Janev et al, 1984). Since we have already considered the balance between equipartition and the sheath losses on electrons we can say that if equipartition is satisfied for sheath losses it will be satisfied for radiation from neutrals. If, as a result of ionisation, T_e is decreased to T < 5 eV, then the radiated energy per new ion pair exceeds the sheath transmission factor per ion pair and the fraction of the heat input to the scrape off layer which impinges on the limiter/divertor plate decreases.

The main effect of ionization is therefore to decrease the temperature in the boundary layer. At low energies, just above the threshold energy the sputtering yield is proportional to energy, thus dividing the same total amount of energy among a large number of ions does not affect the total sputtered flux. However if the temperature can be reduced to a value near or below the sputtering threshold then a significant reduction in the sputtered flux will result.

TABLE 1 Criteria for the Boundary Layer

(i) Parallel field temperature gradients	$\frac{n_s L_c Z_{eff}}{T^2} > 1 \times 10^{17}\ m^{-2}\ eV^{-2}$
(ii) Electron ion equipartition (Sheath dominant)	$\frac{n_e L_c}{T^2} > 1 \times 10^{7}\ m^{-2}\ eV^{-2}$
(iii) Impurity radiation dominant (oxygen and carbon)	$\frac{n_z L_c}{T^{3/2}} > 5 \times 10^{16}\ m^{-2}\ eV^{-3/2}$
(iv) Electron ion equipartition (radiation dominant)	$\frac{n_z}{n_e} < \frac{0.1}{T^{1/2}}$
(v) Ionization determining particle balance	$n_g L_c > 3 \times 10^{18}\ m^{-2}$

3. COMPARISON OF EXPERIMENTAL DATA WITH CRITERIA

The different criteria estimated in section 2 are summarized in Table I. The first four are criteria concerning energy balance, the fifth concerns particle balance. Table II contains data on the boundary layer parameters for a wide range of different tokamaks. Tokamaks using divertors have not been included although the criteria apply equally to these cases. Some earlier data has been given by Zweben and Taylor (1981). In comparing data from different machines account must be taken of the different geometry and different operating conditions of the main plasma. To obtain an estimate of the connection length we have taken the appropriate multiple of the circumference in the case of machines with one or more poloidal limiters. It is then possible to calculate nL_c/T^2. A further difficulty arises because in a number of tokamaks measurements have not been made right to the limiter edge. We have therefore estimated nL_c/T^2 for the actual measured parameters and for the data extrapolated to the limiter edge.

In general the values of nL/T^2 in low field tokamaks are significantly less than $10^{17}\ m^{-2}\ eV^{-2}$. From criteria (i) and (ii) this indicates that we should expect no temperature gradient along field lines nor equipartition of energy between electrons and ions. The two exceptions in table II are TFR 600 and TFTR where values of $2x10^{17}$ and $2x10^{18}\ m^{-2}\ eV^{-2}$ respectively have been obtained in ohmic discharges, primarily due to low edge temperatures. The case of JET is also marginal. All the high field tokamaks FT, Alcator A and Alcator C appear to get well into the conduction limited regime. There appears to be a correlation between machines with high B/R and high nL/T^2, as would be expected from the Murakami parameter. This could be one reason why the measured impurity level in these machines is so low, although as we discuss latter there are other reasons why high density is beneficial.

A further consideration in interpreting this data from different sources is the disturbance of the plasma by the probe. This has been considered in detail in an earlier paper

TABLE II – TOKAMAK EDGE PARAMETERS

TOKAMAK	R m	a m	r_w m	I_p kA	B_T T	$\bar{n}_e$ $10^{19}m^{-3}$	LIMITERS	CONNECTION LENGTHS (m) L_c	EDGE n_e $10^{18}m^{-3}$	EDGE T_e eV	λ_n mm	λ_{T_e} mm	$\frac{N_e L_c}{T^2}$ $10^{17}m^{-2}eV^{-2}$	B/R Tm^{-1}	‡	Ref
TOSCA	0.3	0.08	0.10	8	0.5	1	1 Pol	0.94	0.6	10	11	30	0.06	1.7	M	a
TM3	0.4	0.08	0.12	10–40	1→2.5		1 Pol	1.3	4	30			0.06	6.3	M	b
TCA	0.61	0.18	0.42	75	1.5		1 Pol	1.92	12	10	20	>140	2.3	2.5	E	c
During rf							(Rectangular)		4	25	57	20	0.12	2.5	~10	
JFT2	0.90	0.195	0.29	110	1.7	2.8	1 Rail	8.5	3→5	30–50	14	–	0.21	1.9	M	d
ISXB	0.92	0.26	–	170	1.2	2→4	1 Rail	9–14	2.5	30–40	20	50	0.3	1.3		e
TFR600	0.98	0.19	0.26	–	4	–	1 Pol	3.1	20	18	7	5–10	2	4	E	f
								During rf	5	15–20	14		4	4		
TEXT	1.0	0.27	0.30	100	1.0	0.8	1 Pol	3.1	1.3	17	20	30	0.14	1.0	M	g
									2.5	28			0.1	1.0		
DITE	1.17	0.26	0.30	180	2.1		2 Pol		7	50	20	15	0.3	1.8	E	h
							1 Rail	11	3	20	20	15	0.8	1.8	–	
PLT	1.34	0.40	0.50	–	≈3	2.2	1 Rail	32	0.6	25	25	14	0.3	2.2	~60	i
TEXTOR	1.75	0.46		350	2.0	2.5	4 Rail	11	1	20	10	–	0.3	1.1	M	j
TFTR	2.55	0.83		1400	–	3	2 Rail	30–50	3	8	25	58	14	2.0	~60	k
JET	2.98	1.14	1.33	3400	3.4	3	4 Rail	40	4	50	40	60	0.6	1.1	E	l
ALCATOR A	0.60	0.10		250	6.0	35	1 Pol	1.98	80	12	12	7	11	10	M	m
ALCATOR C	0.64	0.16	0.19	300	6.0	20	2 Pol	1.0	400	15–20	3	–	12	9.4	E	n
									40	12			3	9.4	M	n
FT	0.83	0.20	0.23	300	8.0	3.5	1 Pol	2.6	40	18	5	90	3	9.6	E	p
				500	8.0	17			150	15	4	∞	17	9.6	E	p

‡ M measure at the limiter edge; E extrapolated to the limiter edge. Where the data has not been measured and cannot be extrapolate the distance behind the limiter where the measurements have been made has been noted in mm.

a Howling A et al (1985)
b Bobrovoski G A et al (1977)
c Gimzewski J K et al (1983)
d Gomay Y et al (1978)
e Mioduszewski P (1982)
f Grossman A (1984)
g Ritz C P et al (1984)
h McCracken G M et al (1984)
i Budny R (1982)
j Bogen P et al (1984)
k Kilpatrick S J et al(1985)
l Stangeby P C et al (1985)
m Scatturo L S et al (1978)
n Hayzen A J et al (1981)
p Pericoli V (1984)

(Stangeby, 1985b). If the probe is large then it will behave like a limiter and the results can readily be interpreted provided the resulting change in connection length is taken into account. If the probe is small enough it will measure local plasma parameters. Measurements are then not those close to the limiter. The values of n and T at the limiter will be higher and lower respectively (assuming pressure continuity along the field line). The estimated values of nL_c/T^2 will only be lower limits i.e., the collisionality may be higher.

4. SOURCES OF IMPURITIES

Both the wall and the limiter are sources of impurities. There are quite a large number of potential impurity source mechanisms including sputtering, desorption, evaporation and arcing. Even considering only sputtering the effects of the plasma ions, the impurity ions and the charge exchange neutrals all have to be considered independently. For example the impurity ions, like the main plasma species, will be accelerated by the limiter sheath potential. However if the impurities have been multiply ionized the energy they gain in the sheath will be a multiple of that gained by a singly ionized species. Thus the estimation of the charge state of the impurity ions can be an important part of any modelling.

Although arcing and evaporation can be important mechanisms under some conditions of operation, sputtering normally dominates (McCracken, 1980). Fortunately it is fairly well understood and analytical forms from the yield of sputter atoms per incident ion are available as a function of incident ion energy and angle (Bohdansky, 1984). Thus it can be fairly readily incorporated into models of the plasma boundary. Consider for example the case where impurity influxes from the wall can be neglected compared with the limiter source. A simple particle balance can be written eg., for the impurities from the limiter material.

$$\phi_m = (\phi_p Y_p + \phi_L Y_L + \phi_m Y_m) \tag{14}$$

where Y_p, Y_L and Y_m are the sputtering yield of the plasma ions, oxygen impurity ions and limiter material impurity ions, and ϕ_p, ϕ_L and ϕ_m are the particle fluxes entering the plasma. From equation (14) we obtain

$$\phi_m = \frac{(\phi_p Y_p + \phi_L Y_L)}{1 - Y_m} \tag{15}$$

and hence we see that if $Y_m > 1$ the value of ϕ_m tends to infinity, i.e. there is no steady state solution.

In order to relate the impurity influx to the impurity density in the core plasma a model is required to account for the cross field impurity transport. Neoclassical transport leads in some cases to the conclusion that all impurities are driven to the centre of the plasma and accumulate there. However little experimental evidence has been obtained for this effect. Impurity transport can generally be described by diffusion driven by its own density gradient with a diffusion coefficient of the same order as that for plasma ion transport. A simple model to describe the impurity behaviour in the boundary has been proposed by Englehardt, (1982), and developed by Post and Lackner, (1985). We consider the impurity atoms to be ionized at a single radial position r_i. Two separate cases can be distinguished: $r_i < a$ and $r_i > a$, where a is the limiter radius. Fig. 2 illustrates the two cases. Case I shows that in steady state for $r_i < a$ there is a constant density in the centre, $n_m(o)$, and a constant gradient near the boundary defined by

$$\phi_m = \frac{-D\{n_m(0) - n_m(a)\}}{r_i - a} \tag{16}$$

where D is the impurity diffusion coefficient, $n_m(a)$ is the impurity concentration at the limiter and ϕ_m is the flux density of impurities injected radially. In equation (16) we have ignored any inward transport term, since this is generally small at the boundary.

It is assumed that the impurities, once ionized, distribute themselves uniformly, both poloidally and toroidally. In the boundary region the impurities are lost to the limiter at a volumetric loss rate of $n_m c_s/L_c$. The scrape-off layer thickness for the impurities is $\lambda_m = \sqrt{D_m L_c/c_s}$, and thus

$$\phi_m = n_m(a)\ c_s \int_0^{\ell} \exp(-x/\lambda_m)dx$$

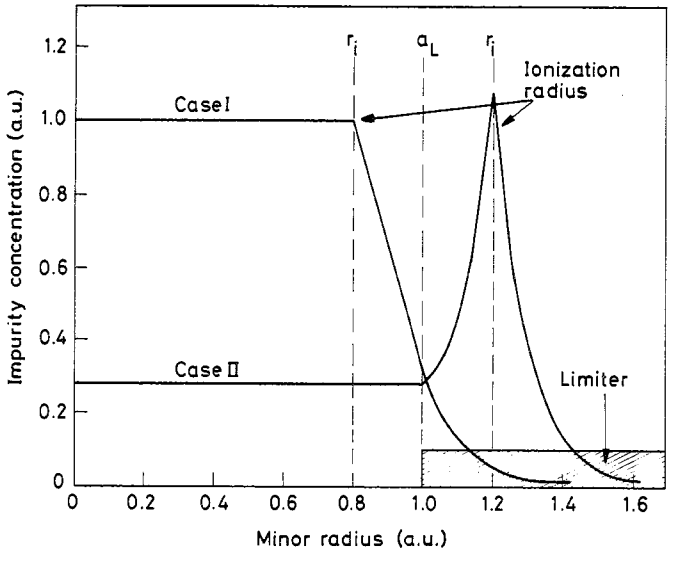

Fig. 2. Schematic diagram of the radial diffusion of an impurity ion. Case I the ionization source is in the region radially inside the limiter. Case II the ionization source is outside the limiter. There is a parallel loss for all radii $\geq a_L$.

If ℓ, the distance to the wall >> λ_m then

$$n_m(a) = \phi_m \lambda_m / D_m$$

and hence

$$n_m(o) = \phi_m \{r_i - a + \lambda_m\} D_m \tag{17}$$

For $r_i > a$ we get the situation shown in Fig. 2, Case II. The impurity concentration peaks outside the limiter radius and falls exponentially on either side of the maximum due to the parallel loss term. The equilibrium concentration within the confined plasma is given by

$$n_m(o) = \phi_m \lambda_m \exp\left[-(r_i - a)/\lambda_m\right] / D_m \tag{18}$$

A number of examples are shown in Fig. 3, where the impurity concentrations varies over orders of magnitude for the same impurity input flux, as the ionization radius is varied.

The relation between the plasma flux and the density can be obtained in an analogous way. Hence equation (14) for the particle balance can be expressed in terms of densities, using only the cross field diffusion coefficients, which can be obtained empirically.

5. SPUTTERING YIELDS

To calculate the value of the sputtering yield we need to know the edge temperature $T_e(a)$. This can be obtained in principle by considering the overall energy balance between the total heating power P_H, the power radiated, P_R and the power conducted and convected out by particles P_c, i.e.

$$P_H - P_R = P_c = k\, T_e(a) \gamma_\perp \phi_p \tag{19}$$

where ϕ_p is the total particle flux to the boundary and $\gamma_\perp$ is the factor determining the energy lost per ion pair crossing the separatrix into the boundary region. We have already

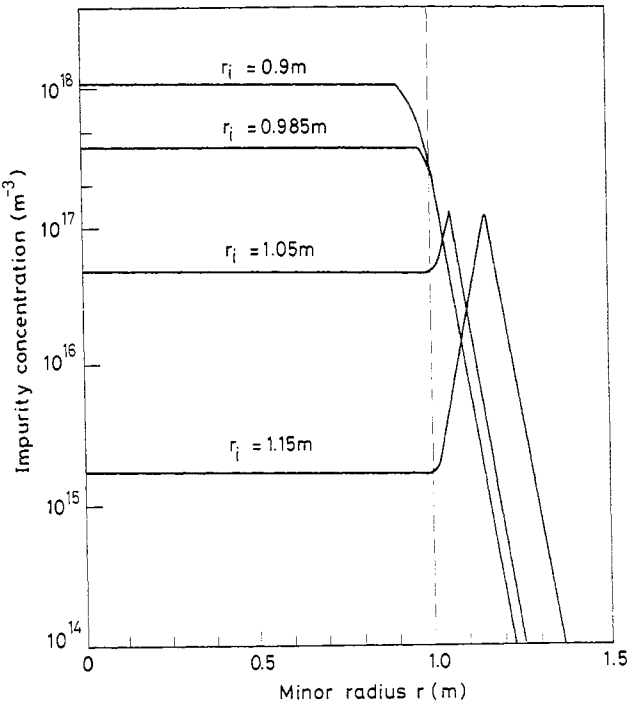

Fig. 3. Impurity concentrations for different ionization radii, illustrating the large difference in central concentrations, depending on ionization radius, for the same influx. A diffusion coefficient of 0.5 m^2 s^{-1} is assumed, and the influx is 5 x 10^{20} atoms s^{-1} over an area of 160 m^2.

defined $\gamma_\parallel$ as the energy transmission factor at the sheath. Generally it is observed that $\gamma_\perp \approx \gamma_\parallel \approx 10$ (Hugill, 1983). The total power radiated can be obtained for example from the average ion model (Post et al., 1977), which assumes coronal equilibrium, if some intelligent guess is made for the plasma density and temperature profiles. In general coronal equilibrium is not reached in the boundary layer and it is more satisfactory to use the time and density dependant radiation factors calculated for example by Carolan and Piotrowitz (1983).

The ion energy is obtained from

$$E = 2kT_i + 3qkT_e \tag{20}$$

where q is the charge state of the ion in the boundary and the factor 3 represents the sheath and presheath acceleration. A simple form for the sputtering yield for a particular ion-atom combination is (Bohdansky et al. 1980).

$$Y = 8.5\ 10^{-5}\ Q(m_1, m_2)\ (E/E_T)^{1/4}(1-E_T/E)^{7/2} \tag{21}$$

where E_T the threshold energy for sputtering, and $Q(m_1,m_2)$ depend on the incident species and target materials only. Reliable values of E_T and Q are available for most species from experiments (Bohdansky et al. (1980), Bohdansky (1984)). From this data and equation (20) Y_p Y_L and Y_m can be obtained. From such a set of equations provided the radiation term P_R can be put in analytical form, we can calculate the impurity concentration as a function of input power and plasma density.

6. PENETRATION OF IMPURITIES INTO THE PLASMA

As can be seen by comparing equations (17) and (18) it is the impurity atoms which penetrate past the separatrix which make the largest contribution to the impurity concentration in the core plasma $n_m(0)$. Therefore impurity ionization within the scrape-off layer is particularly effective in screening the main plasma from impurities.

Let us consider the probability of an atom from the wall being ionized in the boundary layer. A flux of atoms released from the wall will be depleted by successive ionisation events in the plasma and the flux at any position x will be given by

$$F(x) = F_0 \exp\{- \int_0^x - \frac{\overline{\sigma v}}{v_0} n_e(x)\, dx\}$$

where $[\overline{\sigma v}]$ is the ionization rate coefficient, v_0 is the velocity of the neutral atom and x is the distance from the wall. We know that a good approximation to the radial dependence of the density in the boundary layer is an exponential function. Taking the case of an atom moving radially in from the wall and taking x=0 at the wall we may write.

$$n_e(x) = n_e\,(a) \exp\,(-\ell/\lambda_n) \exp\,(x/\lambda_n) \qquad (22)$$

where ℓ is the radial distance between the wall and the limiter or separatrix, λ_n is the e-folding length of the plasma density and $n_e(a)$ is the density at the separatrix. We now make the approximation that $[\overline{\sigma v}]$ is independent of radius. This is quite reasonable in many cases, both because the radial dependance of the temperature is weak and because $[\overline{\sigma v}]$ is only weakly dependant on temperature for temperatures over 20 eV. We thus obtain

$$F(x) = F_0 \exp\,\{- \frac{\lambda_n}{d} \exp\,(-\ell/\lambda_n)\,[\exp\,(x/\lambda_n)-1]\} \qquad (23)$$

where $d = v_0/\{[\overline{\sigma v}].n(a)\}$

The ionisation rate at any point x is given by

$$s(x) = dF/dx = - F_0/d.\exp\,(-\ell/\lambda_n) \exp\,\{x/\lambda_n - \lambda/_n d.\exp\,(-\ell/\lambda_n)[\exp(x/\lambda_n)-1]\} \qquad (24)$$

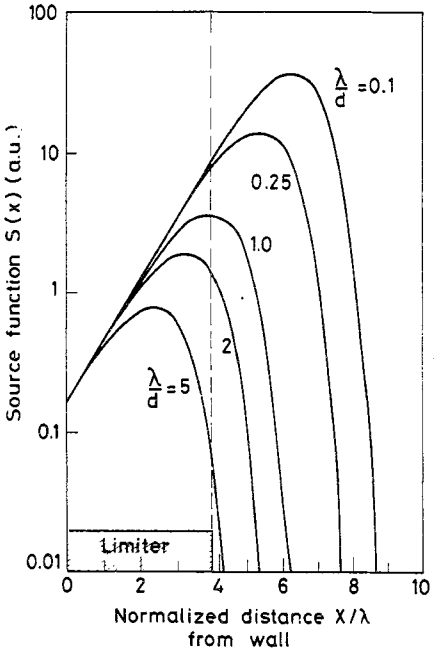

Fig. 4.

The normalised ionization source function calculated from equation (24) for various values of λ/d.

s(x) has a maximum at $x = x_m$ given by

$$x_m = \ell + \lambda \ln(d/\lambda_n) \tag{25}$$

As λ/d decreases the maximum in the ionization rate moves increasingly farther into the plasma. If $\lambda/d > 1$ then the maximum occurs beyond the limiter, in the confined plasma. The use of an exponential density function inside the limiter radius is not normally justified but the criterion for λ/d shows immediately whether the ionization source is predominantly in the boundary layer or not.

The form of s(x), plotted for various values of λ/d, is shown in Fig. 4. This source function can be used instead of the ionization mean free path when calculating the relation between flux and density in the Englehardt model described in section 4. Either the peak of the ionization source function could be taken as a delta function source or, with more difficulty, the whole source function used explicitly, (Englehardt et al., 1982).

Another way of looking at the effect of impurity screening by the boundary is to calculate the fraction of the atoms which actually enter the confined plasma, (although the actual distance they penetrate past the separatrix is also important, equation (17)). The simplest illustration is to calculate the number of atoms which penetrate beyond the limiter edge. The integrated number of atoms ionized outside the limiter radius is obtained from equation (23). The screening efficiency is defined by

$$\eta = 1 - F(\ell)/F(0)$$

$$\text{i.e. } \eta \approx 1 - \exp\left\{-\lambda_n/d \exp\left(-\ell/\lambda_n\right)\left[\exp\left(\ell/\lambda_n\right)-1\right]\right\} \tag{26}$$

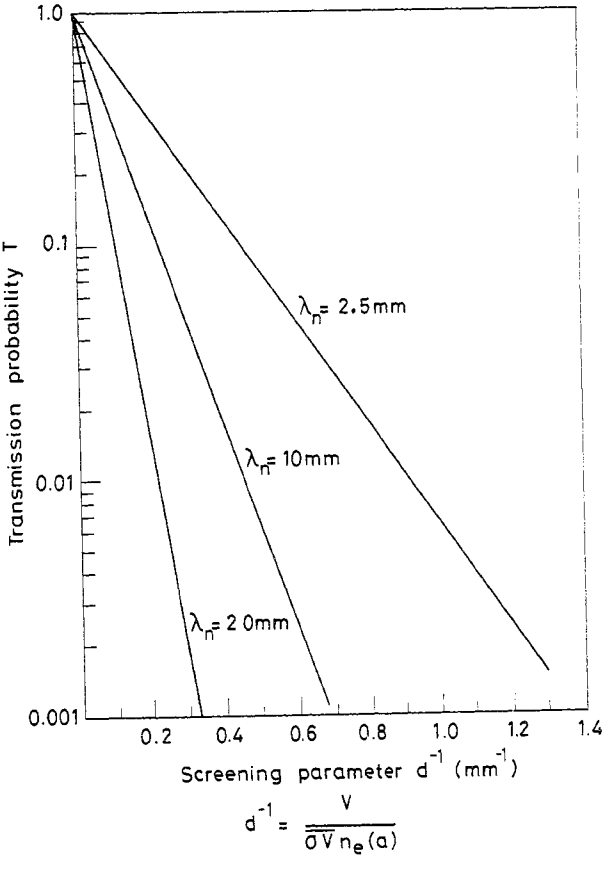

Fig. 5.

Transmission probability for an atom to reach the limiter edge for various values of the screening parameters d. Calculated from equation (27) assuming $1/\lambda_n > 3$.

for $\ell/\lambda > 3$ i.e. $\exp(\ell/\lambda) > 1$ we obtain

$$\eta = 1 - \exp(-\lambda_n/d) \tag{27}$$

The variation of the number of ions reaching the plasma, for $\ell/\lambda > 3$, as a function of λ/d is given in Fig. 5. The parameter $d = v_o/[\overline{\sigma v}]\, n(a)$ is an important measure of the screening, being directly proportional to $1/\eta$ for $\lambda/d < 0.2$.

The above model can in principle be applied to the impurities from the limiter. However the geometry is clearly more complicated since the flux and direction of the sputtered species will depend on the angle of the limiter both for the source term and for the screening

7. COMPARISON WITH EXPERIMENTAL DATA ON IMPURITIES

In real tokamaks there are two clearly separate sources of impurities, those from the wall and those from the limiter. The wall impurities are due primarily to neutral particles ie., photons and charge exchange neutrals atoms, as the plasma density is normally negligible at the wall radius. The charge exchange neutrals can cause sputtering and the photons can cause desorption by direct electronic excitation and by producing photoelectrons (McCracken and Stott, 1979). Although there is not very good quantitative data on the incident fluxes and yields for these two processes there are often direct measurements of the impurity fluxes from the wall. Having experimental measurements of the edge profiles of density and temperature we can calculate the attenuation of the impurity flux from the wall using the analysis of section 6. We take data from JET as an example. Typical JET measured edge profiles of temperature and density (Stangeby et al., 1985) are shown in Fig. 6. The density e-folding length of 40 mm is in agreement with a cross field diffusion coefficient of 0.6 $m^2\ s^{-1}$. The ionization source functions for oxygen, carbon and nickel from the wall have been calculated using the profiles together with equation (24), Fig. 7. Most of ionization occurs at a radius $r > a$. The effective shielding factors given by equation (27) are 86%, 80% and 99% for carbon, oxygen and nickel respectively. It is seen that the shielding for nickel is excellent while for carbon and oxygen it is only partial at the densities and temperatures used.

In the case of the limiter as the impurity source the impurity fluxes depend more critically on the geometry. In order to reduce the power loading at the leading edge, limiters are normally designed with their surfaces at oblique incidence to the magnetic field lines. This means that most impurities being released normal to the surface go directly into the confined plasma. Since the mean free path is very short ($\sim$ 10 mm) for the densities at the limiter edge we can to a first approximation use a constant density and temperature to calculate the profile. The relation between the central density and inward flux is given by equation (16). For JET we use $n_e(a) = 4 \times 10^{18}\ m^{-3}$ and $T_e(a) \simeq 50$ eV. The mean free path for 2 eV carbon atoms is 16 mm, for 2 eV nickel atoms it is 2.6 mm and for 40 eV hydrogen atoms it is 0.88 m. Comparison with Fig. 3 indicates that even for equal fluxes the central concentration of nickel will be considerably lower than for carbon.

Since impurities are normally ionized within a distance shorter than or comparable to λ, it is not necessary to take the precise limiter geometry into account nor to calculate the ionization location precisely: from equation (17) and (18) one has that $n_m(0) \simeq \phi_m \lambda_m / D$ for such a situation. One may also note that the central impurity concentration of each species is simply proportional to the limiter source strength ie., shielding of all species is about the same for all limiter sources (assuming the D and λ are the same for all impurities). For such close-to-limiter ionization, however, the assumption of torioidal/poloidal symmetry does not always hold and the sink action of the scrape-off layer may be localized near the limiter.

Complete self-consistent modelling is beyond the scope of this paper. However it is quite easy to compare the calculated impurity fluxes with those measured spectroscopically. For example in JET the ratios of the fluxes of carbon, oxygen and hydrogen at the limiter have been measured to be typically $\Gamma_C/\Gamma_H = 0.1$ and $\Gamma_O/\Gamma_H = 0.05$ (Stamp et al., 1985). This appears to indicate that the sputtering yield of hydrogen ions on carbon is 0.1 atoms/ion. This is about a factor of four larger than the measured values of physical sputtering (Bohdansky, 1984). Chemical sputtering is almost certainly ruled out as the yield is independent of surface temperature (Roth, 1984). A possible explanation however is that the high yields are due to the sum of plasma ion sputtering, oxygen sputtering and self

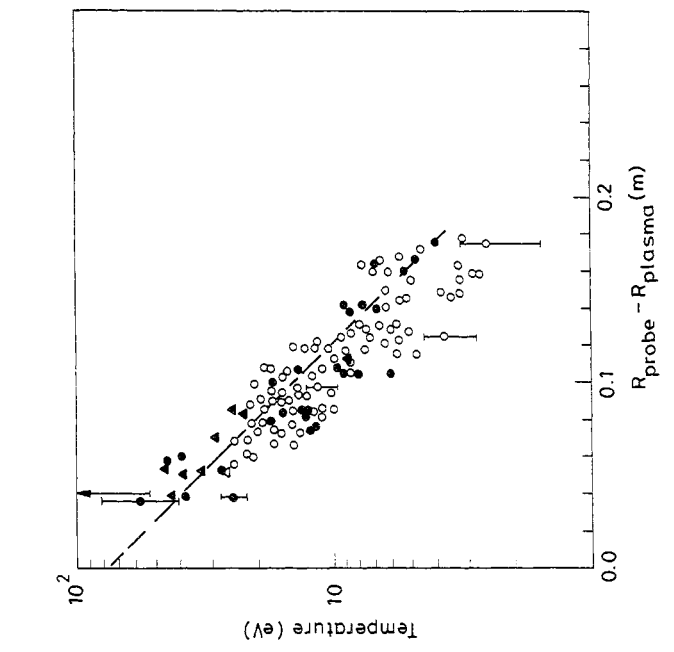

Fig. 6b Electron temperature profile measured in the boundary layer of JET.
$I_p = 3.1$ MA $\int n_e dl = 7 \times 10^{19} m^{-2}$.

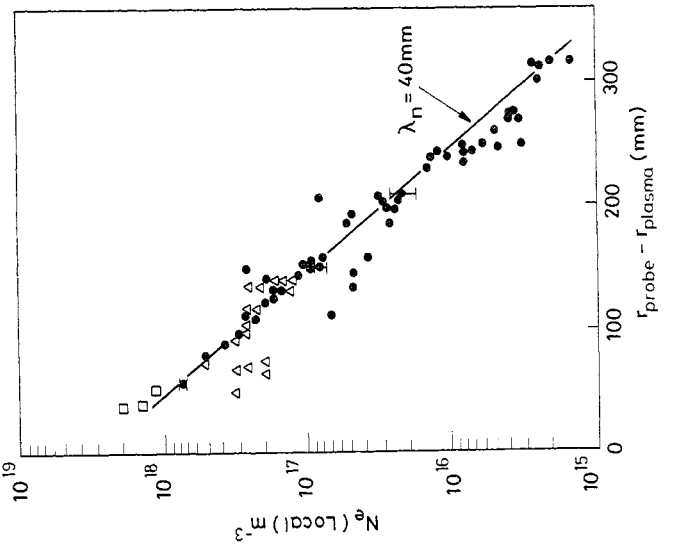

Fig. 6a Density profile measured in the boundary layer of JET.
$I_p = 2.8$ MA $\int n_e dl = 7 \times 10^{19} m^{-2}$.

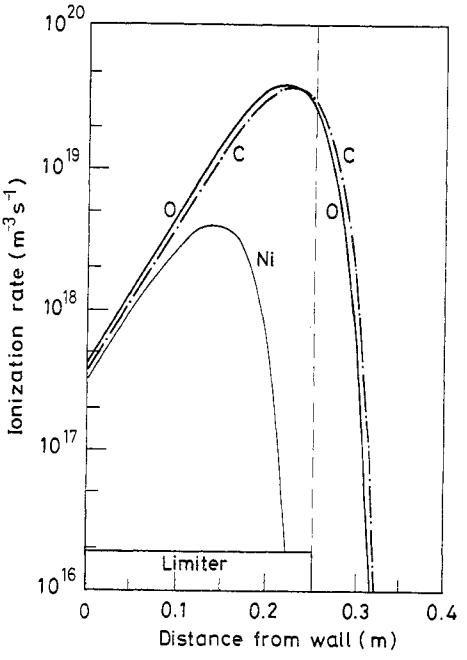

Fig. 7.

Ionization source profiles calculated for wall influxes of nickel, carbon and oxygen using equation (24) and using the experimental density profile from fig. 6a with a constant electron temperature of 20 eV.

sputtering of carbon. From equation (15) the sputtering yields give

$$\frac{\phi_c}{\phi_D} = \frac{Y_{DC} + fY_{o-c}}{1 - Y_{c-c}} = 0.1$$

where f is the fractional impurity flux of oxygen. From the measured edge temperature we can calculate the sputtering yields and hence obtain the expected flux ratio. In fact the yields are not very sensitive to energy in the energy range of interest. It is interesting to compare the relative contribution to the sputtering of the three species.

$$\phi_c = 1 \times 0.025 \text{ (deuterium)} + 0.05 \times 1\text{(Oxygen)} + 0.1 \times 0.35 \text{ carbon)}$$
$$= 0.11$$

It appears that the sputtering of oxygen on carbon has the dominant effect, and thus that a reduction in the oxygen concentration should bring about a significant reduction in the carbon concentration also. At present there is no direct evidence that this effect occurs, and in fact there is some apparently contradictory evidence. This may be due to the fact that a reduction in oxygen content reduces radiative cooling of the edge and increases the hydrogen and carbon sputtering. Further studies are in progress to elucidate this matter.

8. CONCLUSION

The boundary layer is a complex interactive system involving atomic physics and surface physics reactions together with plasma physics transport processes. The extent of the interaction of the plasma with the wall and limiter determines the impurity flux into the plasma. This interaction is determined by the edge conditions and the impurity influx can be affected markedly by whether there is high edge temperature, whether there is a temperature gradient along field lines and whether the ion temperature is greater than the electron temperature.

In order to determine the impurity concentration from the impurity influx it is necessary to have a model of impurity transport in the edge. Englehardt's model of diffusion provides a convenient and physically simple picture of this impurity transport which is in good qualitative agreement with experimental observation. It does not take into account the various complexities of turbulence and ergodicity frequently mentioned in connection with edge behaviour. However it uses an empirical value of the diffusion coefficient which to first order makes allowance for these complexities. This diffusion model makes clear that

the central impurity concentration is not related to impurity production rate alone. High plasma edge densities lead to lower mean free paths for ionization and hence lower central impurity concentrations. In the case of impurities from the wall, ionization can lead to impact of the ions on the inside of the limiter thus making little contribution to the central impurity concentration. Even in the case of impurity atoms from the limiter entering directly into the confined plasma a short ionization mean free path will significantly reduce the ratio of the impurity concentration to the impurity influx. It is possible in principle to change from low density conditions where impurities from the wall dominate, to high density where only the limiter produced impurities play a significant role. If we take into account that, for a given power input, high edge densities also reduce the edge temperature the importance of achieving high edge densities becomes increasingly clear. The low impurity levels observed in high field tokamaks strongly support this general picture. The only way known at present to attain high densities is to have high toroidal field and/or a small major radius.

REFERENCES

Bobrovoski G.A., and Kondratev A.A., Fiziky Plasmy 3 (1977) 209.

Bogen P., Hartwig H., Hintz E., Hothker K., Lie Y.T., Pospieszczyk A., Samm U., and Bieger W. J. Nucl. Mat. 128 and 129 (1984) 157.

Bohdansky J., Nuclear Fusion Supplement (1984), 61.

Bohdansky J., Roth J. and Bay H.L., J.Appl.Phys. 51 (1980) 2861.

Budny R., J Vac. Sci and Tech. 20 (1982) 1238.

Carolan P.G., and Piotrowicz V.A., Plasma Physics 25 (1983) 1065.

Englehardt W. et al., J.Nucl.Mat. 111 and 112 (1982) 337.

Gimzewski J.K., Hofmann F., Hollenstein C., Joye B., Lietti A., Lister J.B., Pochelon A., and Veprek S. Scrape-off measurements during Alfven wave heating in the T.C.A. tokamak. CRPP Lausanne Report LRP 226/83 (1983).

Gomay Y., Fujisawa N., Maeno M., Suzuki N., Uehara K., Yamamoto T., Konoshima S. Nuclear Fusion 18 (1978) 849.

Grossman A. Private communication 1984.

Hayzen A.J., Overskei D.O., and Moreno J. Probe measurements in the boundary plasma in ALCATOR C. MIT Report PFC/JA-81-19 1981.

Howling A., Coté A., Doyle E.J., Evans D.E., and Robinson D.C. Proceedings of the 12th E.P.S. Conf. on Controlled Fusion and Plasma Physics. Budapest 1 (1985) 311, and Howling A., Private communication 1984.

Hugill J., Nuclear Fusion., 23 (1983) 331.

Janev R.K., Post D.E., Langer W.D., Evans K., Heifitz D.B., and Weisheit J.C., J. Nucl. Mat. 121 (1984) 10.

Kilpatrick S.J., Manos D.M., and Stangeby P.C. Bull. of the A.P.S. 29 (1984) 1310.

Lackner K. and Post D.E, NATO Advanced Study Institute on The Physics of Plasma Wall Interaction in Controlled Fusion, Val Morin, Canada, 1984. to be published by Plenum Press.

McCracken G.M., J.Nucl.Mat 93 and 94 (1980) 3.

McCracken G.M., and Stott P.E., Nuclear Fusion 19 (1979) 889.

McCracken G.M., Erents S.K., Goodall D.H.J., Matthews G.F., Partridge J.W., Fielding S.F., and Powell B.A. J. Nucl. Mat. 128 and 129 (1984) 150.

Mioduszewski P., J. Nucl. Mat. 111 and 112 (1982) 253.

Pericoli-Ridolfini V., Private communications 1984.

Post D.E., Jensen R.V., Tartar C.B., Grasberger W.H., and Lokke W.A., At.Data.Nucl.Data Tables 20 (1977) 397.

Ritz C.P., Bengston R.D., Levinson S.J., and Powers E.J. Phys Fluids 27 (1984) 2956.

Roth J., Nuclear Fusion Supplement (1984) 72.

Scatturo L.S., and Kuss B. Nuclear Fusion 18 (1978) 1717.

Spitzer L., "Physics of fully ionized gases" J. Wiley and Sons Inc. New York, 1962.

Stamp M.F., Behringer K.H., Forest M.J., Morgan P.D., and Summers H.P., Proceedings of the 13th European Physical Society meeting on Plasma Physics and Nuclear Fusion, Budapest 1985, to be published.

Stangeby P.C., Erents S.K., Tagle J.A., McCracken G.M., and de Kock L. Proceedings of the 12th E.P.S. Conf on Controlled Fusion and Plasma Physics, Budapest 2, (1985) 187.

Stangeby P.C., Phys. of Fluids 27 (1984) 682.

Stangeby P.C., Phys of Fluids 28 (1985a) 644.

Stangeby P.C. J. Phys D., in press (1985b).

Stangeby P.C., Erents S.K., Tagle J.A., McCracken G.M., de Kock L., 13th European Physics Society Meeting on Plasma Physics, Budapest, September 1985.

Zweben S.J. and Taylor R.J. UCLA Report, PPG 463 (1980).